Neurobiology of Disease

The Divergent Roles of Dietary Saturated and Monounsaturated Fatty Acids on Nerve Function in Murine Models of Obesity

Amy E. Rumora,[1] Giovanni LoGrasso,[1] John M. Hayes,[1] Faye E. Mendelson,[1] Maegan A. Tabbey,[1] Julia A. Haidar,[1] Stephen I. Lentz,[2] and Eva L. Feldman[1]

Departments of [1]Neurology, and [2]Internal Medicine, University of Michigan, Ann Arbor, Michigan 48109

Neuropathy is the most common complication of prediabetes and diabetes and presents as distal-to-proximal loss of peripheral nerve function in the lower extremities. Neuropathy progression and disease severity in prediabetes and diabetes correlates with dyslipidemia in man and murine models of disease. Dyslipidemia is characterized by elevated levels of circulating saturated fatty acids (SFAs) that associate with the progression of neuropathy. Increased intake of monounsaturated fatty acid (MUFA)-rich diets confers metabolic health benefits; however, the impact of fatty acid saturation in neuropathy is unknown. This study examines the differential effect of SFAs and MUFAs on the development of neuropathy and the molecular mechanisms underlying the progression of the complication. Male mice *Mus musculus* fed a high-fat diet rich in SFAs developed robust peripheral neuropathy. This neuropathy was completely reversed by switching the mice from the SFA-rich high-fat diet to a MUFA-rich high-fat diet; nerve conduction velocities and intraepidermal nerve fiber density were restored. A MUFA oleate also prevented the impairment of mitochondrial transport and protected mitochondrial membrane potential in cultured sensory neurons treated with mixtures of oleate and the SFA palmitate. Moreover, oleate also preserved intracellular ATP levels, prevented apoptosis induced by palmitate treatment, and promoted lipid droplet formation in sensory neurons, suggesting that lipid droplets protect sensory neurons from lipotoxicity. Together, these results suggest that MUFAs reverse the progression of neuropathy by protecting mitochondrial function and transport through the formation of intracellular lipid droplets in sensory neurons.

Key words: **diabetes; monounsaturated fatty acid; neuropathy; prediabetes; saturated fatty acid; sensory neuron**

Significance Statement

There is a global epidemic of prediabetes and diabetes, disorders that represent a continuum of metabolic disturbances in lipid and glucose metabolism. In the United States, 80 million individuals have prediabetes and 30 million have diabetes. Neuropathy is the most common complication of both disorders, carries a high morbidity, and, despite its prevalence, has no treatments. We report that dietary intervention with monounsaturated fatty acids reverses the progression of neuropathy and restores nerve function in high-fat diet-fed murine models of peripheral neuropathy. Furthermore, the addition of the monounsaturated fatty acid oleate to sensory neurons cultured under diabetic conditions shows that oleate prevents impairment of mitochondrial transport and mitochondrial dysfunction through a mechanism involving formation of axonal lipid droplets.

Introduction

Type 2 diabetes (T2D) is a prevalent and debilitating disease, affecting >30 million Americans (Callaghan et al., 2015). Another 80 million Americans have prediabetes and one-third of these individuals will progress to T2D (Tabák et al., 2012). Prediabetic and type 2 diabetic patients exhibit similar metabolic risk factors, including obesity and dyslipidemia, and develop the same microvascular and macrovascular complications (Callaghan et al., 2012a, 2016b). The most common microvascular

Received Dec. 18, 2018; revised Jan. 23, 2019; accepted Feb. 8, 2019.

Author contributions: A.E.R., S.I.L., and E.L.F. designed research; A.E.R., G.L., J.M.H., F.E.M., M.A.T., and J.A.H. performed research; A.E.R., G.L., J.M.H., and S.I.L. analyzed data; A.E.R. wrote the first draft of the paper; A.E.R. wrote the paper; S.I.L. and E.L.F. edited the paper.

This work was supported by U.S. National Institutes of Health (NIH) National Institute of Diabetes and Digestive and Kidney Diseases (NIDDK) Grants R24 DK082841 and R01 DK107956 (to E.L.F.) and F32 1F32DK112642 and T32 1T32DK101357 (to A.E.R.); the NIDDK DiaComp Award DK076169 (to E.L.F); Novo Nordisk Foundation Grant NNF140C0011633 (to E.L.F.); the Milstein, Nathan, and Rose Research Fund; the Michigan Mouse Metabolic Phenotyping Center supported by NIH Grant U2C; the American Diabetes Association; the Program for Neurology Research and Discovery; and the A. Alfred Taubman Medical Research Institute. Confocal microscopy and image analysis were completed at the Michigan Diabetes Research Center's Microscopy and Image Analysis Core, supported by NIH NIDDK Grant P60DK020572. We thank Shayna Mason for conducting animal experiments, Erin Reasoner for data analysis contributions, Dr. Stacey Sakowski Jacoby and Dr. Sami Narayanan for their expert editorial advice, and Dr. Ahmet Hoke (Johns Hopkins University, Baltimore, MD) for the gift of the 50B11 DRG neurons.

The authors declare no competing financial interests.

Correspondence should be addressed to Eva L. Feldman at efeldman@umich.edu.

https://doi.org/10.1523/JNEUROSCI.3173-18.2019

complication is peripheral neuropathy that results in distal-to-proximal loss of sensation in the limbs due to injury of sensory myelinated and unmyelinated nerve fibers. The progression of peripheral neuropathy in prediabetes and T2D correlates with dyslipidemia (Smith et al., 2006; Callaghan et al., 2012b; Cortez et al., 2014). Elevated levels of circulating triglycerides and free fatty acids associated with dyslipidemia result from high-fat diets (HFDs) containing elevated levels of saturated fatty acids (SFAs; German and Dillard, 2004). To identify mechanisms underlying neuropathy progression in prediabetes and T2D, our laboratory established a model of neuropathy in C57BL/6J mice fed a lard-based HFD rich in SFAs (O'Brien et al., 2014; Hinder et al., 2017). These obese, insulin resistant and hyperlipidemic mice develop neuropathy with reduced motor and sensory nerve conduction velocities (NCVs) and decreased intraepidermal nerve fiber densities (IENFDs), similar to neuropathy in prediabetic and T2D humans. Neuropathy progression is reversed by changing mice from a HFD to a standard diet, restoring nerve function, body weight, and glucose tolerance (Hinder et al., 2017; O'Brien et al., 2018). Therefore, excess dietary SFAs associated with prediabetes and T2D may contribute to the progression of peripheral nerve damage (Hagenfeldt et al., 1972; Fraze et al., 1985; Miles et al., 2003).

Peripheral nerves are composed of nerve fibers that contain bundles of axons from sensory dorsal root ganglion (DRG) neurons. DRG neurons are dependent on mitochondrial ATP production throughout the axon and rely on mitochondrial transport mechanisms to distribute mitochondria for normal nerve function (Schwarz, 2013; Sheng, 2014). DRG neurons exposed to elevated levels of SFAs exhibit a decrease in motile axonal mitochondria (Rumora et al., 2018, 2019). This SFA-induced impairment of mitochondrial transport is accompanied by mitochondrial depolarization and impaired mitochondrial bioenergetics (Rumora et al., 2018). Dysfunctional bioenergetics lowers the level of intracellular ATP and initiates DRG apoptosis (Rumora et al., 2019). These studies indicate that lipotoxic SFAs impair mitochondrial function and play a critical role in peripheral neuropathy progression.

Dietary intervention studies whereby SFAs are replaced with monounsaturated fatty acids (MUFAs) reverse the adverse effects of SFAs in prediabetes and T2D. MUFAs can lower insulin resistance, normalize plasma triglycerides, and improve metabolic risk factors associated with prediabetes and T2D (Qian et al., 2016; Wanders et al., 2017). At a cellular level, MUFAs modulate mitochondrial function and improve lipid homeostasis (Burhans et al., 2015; Ducheix et al., 2017) by upregulating the expression of genes related to mitochondrial oxidative pathways (Das et al., 2010; Henique et al., 2010). This stimulation of lipid oxidation increases mitochondrial ATP production (Burhans et al., 2015). Additionally, MUFAs stimulate triglyceride formation to sequester SFAs into neutral lipid droplets, thereby limiting lipotoxicity and apoptosis in hepatocytes, adipocytes, skeletal muscle, and β-cells (Thörn and Bergsten, 2010; Kwon et al., 2014; Capel et al., 2016). However, the impact of dietary MUFAs on neuropathy and sensory neuron mitochondrial function is unknown.

We evaluated the effect of dietary MUFAs on neuropathy progression and identified underlying molecular effects of MUFAs on mitochondrial transport and function in DRG neurons. Switching mice from a SFA-rich HFD to a MUFA-rich HFD restored nerve function in obese mice with neuropathy. We next evaluated the mechanisms underlying dietary MUFA supplementation and discovered that MUFAs prevent SFA-induced impairment of axonal mitochondrial transport and function, likely via the formation of intra-axonal lipid droplets. These findings provide insight into the efficacy of MUFA-based diets and suggest that dietary intervention is a plausible strategy to treat neuropathy.

Materials and Methods

Mouse studies. Fifteen-week-old male C57BL/6J mice fed either a standard diet (stock #380056) or 60% SFA-rich HFD (stock #380050) from 6 weeks of age were purchased from The Jackson Laboratory. At 16 weeks of age, mice were divided into three groups: (1) SD mice maintained on a standard diet (D12450B: 10% kcal fat, Research Diets) until 24 weeks of age ($n = 5$/group), (2) HFD mice fed a lard-based 60% HFD (D12492: 60% kcal fat, Research Diets) until 24 weeks of age ($n = 7$/group), and (3) HFD-MUFA mice fed a lard-based 60% HFD until 16 weeks of age followed by a MUFA-based 60% HFD (D18043009: 60% kcal fat derived from high MUFA sunflower oil, Research Diets) from 16 to 24 weeks of age ($n = 8$/group). The fatty acid composition of the SD, HFD, and HFD-MUFA is provided in Fig. 1-1, available at https://doi.org/10.1523/JNEUROSCI.3173-18.2019.f1-1. All animals were housed in a pathogen-free environment at the University of Michigan. Animal work protocols adhered to the University of Michigan, state, and federal guidelines accredited by the Association for the Assessment and Accreditation of Laboratory Animal Care International. Protocols were approved by the University of Michigan Institutional Animal Care and Use Committee (Protocol PRO00008115).

Metabolic and neuropathy phenotyping. At the termination of the study, mouse body weights were collected and body composition parameters, including lean mass, fat mass, and body fluids, were assessed using an NMR-based Bruker Minispec LF 9011 at the University of Michigan Mouse Metabolic and Phenotyping Core. A terminal glucose tolerance test was completed by measuring fasting blood glucose using an Alpha-Trak Glucometer (Abbott Laboratories). This was followed by administration of a glucose bolus at 1 g/kg body weight via intraperitoneal injection for each mouse and blood glucose levels were monitored for 2 h after administration of the glucose bolus.

Neuropathy phenotyping included sural nerve and motor NCVs and footpad IENFD measurements. All neuropathy phenotyping was completed according to guidelines of the Diabetic Complications Consortium (https://www.diacomp.org/shared/protocols.aspx; Oh et al., 2010). To evaluate IENFD, footpads were extracted from the plantar surface of the hindpaw, fixed, embedded, and stained according to (Cheng et al., 2012). Fluorescent *z*-series images were captured at an optical thickness of 3.3 μm using an Olympus FV500 confocal microscope (20× objective, 1024 × 1024 pixel resolution). Nerve fibers that crossed the basement membrane into the epidermis in each *z*-series were examined and quantified using MetaMorph v7.7.0.8 (Molecular Devices; RRID: SCR_002368; Hinder et al., 2017).

Primary DRG neuron cell culture. Primary DRG neuron cultures were used to evaluate the effect of oleate and palmitate fatty acid treatments on axonal mitochondrial transport, mitochondrial membrane potential (MMP) and lipid droplet formation. DRG neurons from adult 16- to 18-week-old male C57BL/6J mice (The Jackson Laboratory) were dissected and cultured as described in our previously published protocols (Vincent et al., 2007, 2009a,b; Rumora et al., 2018, 2019). Briefly, intact DRG were incubated in 2 mg/ml collagenase (Millipore-Sigma) for 30 min at 37°C. The DRG were then mechanically dissociated in heat-inactivated bovine serum albumin (BSA) using repetitive trituration. DRG neurons were resuspended in treatment media (TM; 50% F-12K; Cell Gro, Corning) and 50% DMEM (Cell Gro, Corning), 1:100 dilution of Nb^+, 1000 U/ml penicillin/streptomycin/neomycin (ThermoFisher Scientific), 7.2 μM aphidicolin (Millipore-Sigma), supplemented with 1× B27 and 0.4 μM L-glutamine (Rumora et al., 2018, 2019) and transfected with mitochondria-GFP by adding 3.75 μl/ml CellLight mitochondria-GFP (mito-GFP BacMam 2.0, ThermoFisher Scientific). The DRG neurons were then plated on 4-well Nuc Lab-Tek chambered cover glass imaging plates (ThermoFisher Scientific) coated with 25 μg/ml laminin (Millipore-Sigma). After 24 h, the DRG neuron culture media was replaced with feed media composed of TM and 1× B27 sup-

plement for another 24 h allowing for DRG axon outgrowth (Rumora et al., 2018, 2019).

Fatty acid treatments. Fatty acid preparation: oleate (Millipore-Sigma) and palmitate (Nu-Chek Prep) fatty acids were conjugated to fatty acid-free BSA (ThermoFisher Scientific) at 5 mM fatty acid concentration (Rumora et al., 2018). The 5 mM stock of oleate and palmitate was used to prepare the required oleate and palmitate treatments. *Oleate and palmitate treatments*: primary DRG neurons were treated with physiological concentrations ranging from 31.25 to 250 μM of the SFA palmitate, or 31.25–250 μM of the MUFA oleate, for 24 h. To quantitate the basal percentage of motile mitochondria in DRG neurons without fatty acid treatment, a TM control was used, and to identify whether BSA alone had an effect on mitochondrial transport in DRG neurons, a 0.25% BSA vehicle control was used. DRG neurons were also treated with oleate/palmitate mixtures at a 1:1 equimolar or 2:1 molar ratio to determine the impact of mixtures on mitochondrial transport and function. Last, to determine whether oleate could rescue mitochondrial transport in DRG neurons treated with palmitate, cultures were treated with palmitate treatments for 12 h followed by two rinses with TM and a 12 h incubation with oleate. The ability of oleate to prevent palmitate-induced inhibition of mitochondrial transport was evaluated by pre-treating DRG neurons with oleate for 12 h, washing the cells twice with TM, and then replacing the treatment with palmitate.

Mitochondrial trafficking and kymograph analysis. Mitochondrial trafficking analyses were performed with live-cell time-lapse microscopy on a Nikon A1 confocal microscope (Nikon Instruments) as described previously (De Vos et al., 2007; Rumora et al., 2018). Mitochondrial transport in the axon of each DRG neuron was recorded using a 40× objective and confocal aperture setting at 4.49 μm optical thickness. Consecutive images were taken 2.5 s apart for 2.5 min with NIS Elements ND acquisition software. Throughout the image acquisition, live DRG neurons were maintained at 5% CO_2 and 37°C in a Tokai Hit environmental chamber.

DRG neuron mitochondrial trafficking was assessed using kymograph analysis with MetaMorph software (Molecular Devices) as described previously (Rumora et al., 2018). For each neuron, a region of interest was drawn down the axon away from the cell body and mitochondrial signals within 10 μm of that region of interest were incorporated into the kymographing analysis. Two kymographs were generated to identify the number of motile and stationary mitochondria (De Vos et al., 2003, 2007; De Vos and Sheetz, 2007; Rumora et al., 2018), and the percentage of stationary and motile mitochondria was derived from the kymographs. Mitochondria that were transported at a velocity lower than the threshold velocity of 0.02 μm/s were categorized as stationary (De Vos et al., 2007).

Mitochondrial depolarization analysis. The impact of oleate and palmitate treatments on MMP was evaluated using the cationic fluorophore, tetramethylrhodamine methyl ester (TMRM; ThermoFisher Scientific; Russell et al., 2002; Vincent et al., 2007). DRG neurons expressing mito-GFP were treated with TM, 0.25% BSA, 125 μM palmitate, 125 μM oleate, 250 μM oleate, and a 1:1 oleate–palmitate mixture for 24 h and then stained with 50 nM TMRM for 30 min at 37°C. Image acquisition and analysis were completed as described previously (Rumora et al., 2018, 2019). An average of 34 neurons from 3 experimental replicates were analyzed for each treatment condition.

50B11 DRG neuron cell culture. A 50B11 DRG neuron immortalized cell line (RRID:CVCL_M745) was used to evaluate the effect of oleate and palmitate on apoptosis and ATP production. The 50B11 DRG neurons were cultured and prepared according to a previously published protocol (Chen et al., 2007; Rumora et al., 2018). Briefly, 50B11 DRG neurons were added to a 96-well plate at a density of 10,000 cells per well in 50B11 media (Neurobasal media, Invitrogen) supplemented with 10% (v/v) heat inactivated fetal bovine serum (Invitrogen), 0.2% glucose (v/v), 0.5 mM L-glutamine (Invitrogen), and 5.6× B27 (Invitrogen). Twelve hours before treatment, the media was changed to TM (50B11 media containing 75 μM forskolin) to differentiate the cells. For the treatment, 75 μM forskolin was added to the TM control, the 0.25% BSA control, and the fatty acid treatments to ensure that the 50B11 DRG neurons remained differentiated throughout the treatment.

CellTiter-Glo and Caspase 3/7-Glo assays. Differentiated 50B11 DRG neurons were treated with 31.25–250 μM oleate or 31.25–250 μM palmitate and mixtures of oleate/palmitate at 1:1 and 2:1 molar ratios in triplicate for 24 h. A CellTiter-Glo assay (Promega) or Caspase 3/7-Glo assay (Promega) was used to assess ATP levels or apoptotic activation in treated 50B11 DRG neurons, respectively, according to the manufacturer's protocols. The luminometric reactions were evaluated on a Synergy| HTX multimode plate reader (BioTek) with Gen5 software v3.03. The luminometric signal, which is measured in relative light units (RLU), was analyzed in an average of six wells of treated 50B11 neurons per condition in two experimental replicates for the CellTiter-Glo assay and three wells of treated 50B11 neurons per condition in one experimental replicate for the Caspase 3/7-Glo assay.

Axonal lipid droplet analysis. The formation of axonal lipid droplets in response to fatty acid treatments was evaluated using Nile red stain to selectively label intracellular lipid droplets (Greenspan et al., 1985; Rumin et al., 2015). Mito-GFP-transfected DRG neurons were treated with 0.25% BSA, 125 μM palmitate, 125 μM oleate, and a 1:1 and 2:1 molar ratio mixture of oleate–palmitate for 24 h. The 0.25% BSA condition was used as the vehicle control to show the level of lipid droplet formation in DRG neurons without fatty acid treatment. The TM condition was excluded from the lipid droplet analysis because of high nonspecific background staining of Nile red. Following 24 h of treatment, 10× Nile red was added to each DRG neuron culture for 30 min at 37°C. The Nile red-containing treatments were then removed from the DRG neurons, the cells were washed 2× with TM to remove excess Nile red, and the treatment was replaced. Single sequential images of DRG neurons exhibiting both mito-GFP and Nile red fluorescence were captured on a Nikon A1 confocal microscope with a 40× objective. The number of axonal lipid droplets and mitochondria were counted using the MetaMorph Image Analysis program (Molecular Devices). For each neuron, the regions of the neurite were selected using the box tool to evaluate lipid droplet accumulation. The Imaris Spots function was used, with an estimated XY diameter of 2 μm, to mark/detect mitochondria and lipid droplets separately along the axon. After adjusting the threshold and changing the color of each different type of spot, mitochondria and lipid droplet spots were quantified and evaluated for colocalization. An average of 32 DRG neurons from 3 experimental replicates were evaluated for lipid droplet formation in each treatment condition.

Experimental design and statistical analysis. Statistical analyses of all datasets were obtained with Prism v7 (GraphPad Software; RRID: SCR_002798). For *in vivo* studies including glucose tolerance tests, body weight, NCVs, and IENFDs, data were collected from 5 to 8 mice per group and plotted as means ± SEM. Statistical significance was evaluated using a one-way ANOVA and Tukey's *post hoc* test for multiple comparisons. NCVs were significant at $^*p < 0.0001$ and IENFDs reached significance at $\#p = 0.0071$ and $\&p = 0.0297$.

All assays evaluating mitochondrial trafficking, mitochondrial depolarization, ATP level, and caspase 3/7 activity in DRG neurons are reported as means ± SEM. Significance was evaluated using a one-way ANOVA and Tukey's *post hoc* test for multiple comparisons. Mitochondrial trafficking results were based on 16–23 DRG neurons treated with 31.25–250 μM oleate alone, 18–23 neurons treated with 1:1 and 2:1 oleate + palmitate mixtures, and 12–16 neurons in oleate rescue experiments. Mitochondrial depolarization analyses included an average of 34 neurons per condition. Results of mitochondrial trafficking and mitochondrial depolarization analyses were statistically significant at $^*p < 0.0001$. CellTiter-Glo ATP assay measurements were performed on six wells per fatty acid treatment condition of 50B11 DRG neurons. A total of three wells of 50B11 DRG neurons were evaluated using the Caspase 3/7-Glo assay for apoptosis. CellTiter-Glo and Caspase 3/7-Glo experiments were statistically significant at $^*p < 0.0001$ and $\#p = 0.0056$. Lipid droplet formation was evaluated in 20–47 DRG neurons and DRG neurons (20–37 neurons) with lipid droplets were assessed for lipid droplet-mitochondrial interactions. Results were statistically significant at $^*p < 0.0001$.

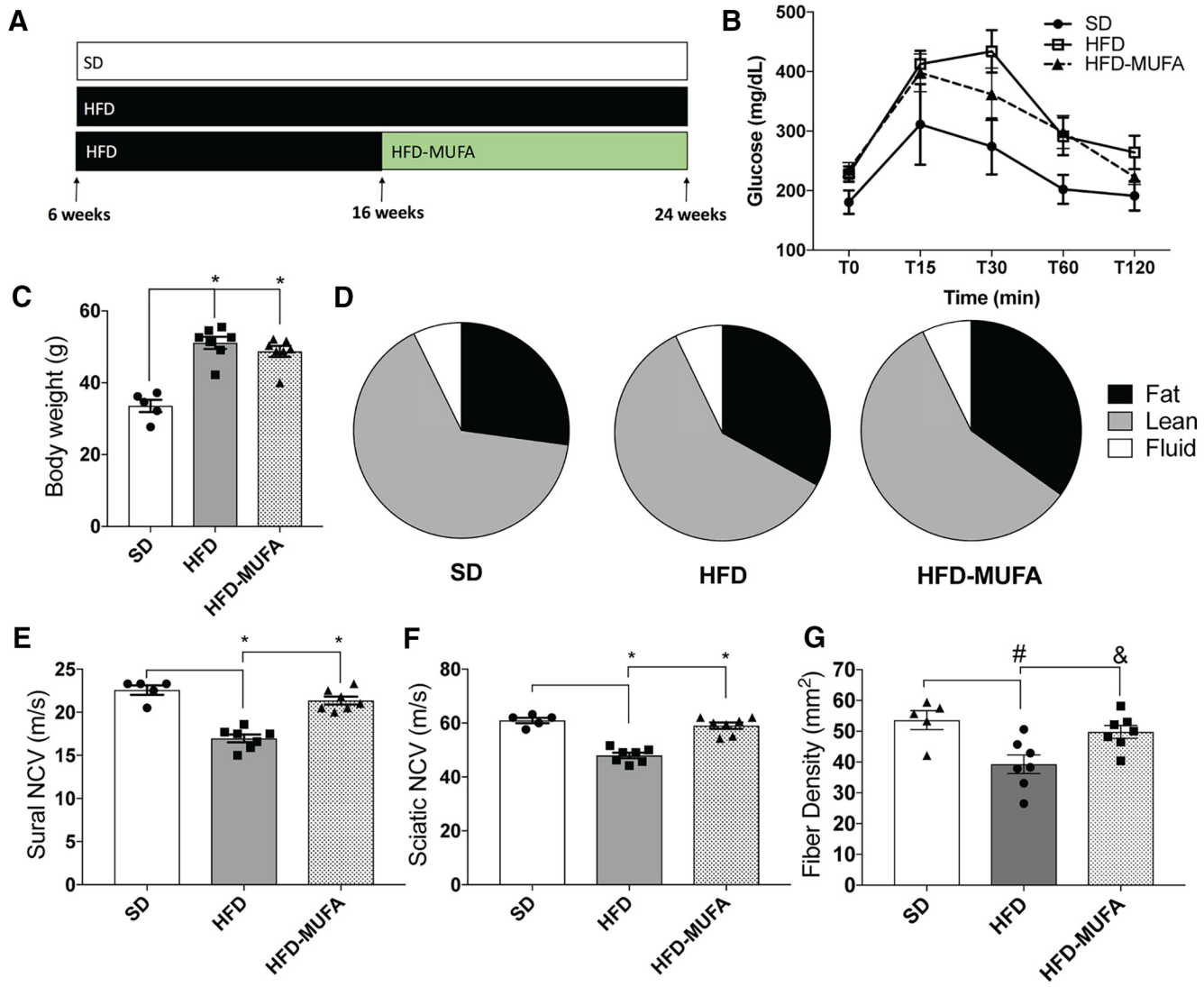

Figure 1. A MUFA-rich diet reverses neuropathy in prediabetic mice. ***A***, Dietary intervention murine model whereby C57BL/6J mice were fed a SD, 60% HFD, or 60% HFD followed by 60% HFD-MUFA (Figure 1-1, available at https://doi.org/10.1523/JNEUROSCI.3173-18.2019.f1-1). ***B–D***, Metabolic phenotyping of mice at 24 weeks of age, including (***B***) glucose tolerance test (mg/dl), (***C***) terminal body weight (g), and (***D***) terminal body composition. ***E***, ***F***, Neuropathy phenotyping using NCV (m/s) for sural and sciatic nerves, respectively (Figure 1-2, available at https://doi.org/10.1523/JNEUROSCI.3173-18.2019.f1-2). ***G***, IENFD of mouse footpad. All data represent mean ± SEM from 5 to 8 animals per group. One-way ANOVA with Tukey's multiple-comparisons test. $*p < 0.0001$, $\#p = 0.0071$, $\&p = 0.0297$.

Results

A MUFA-rich diet restores nerve function

We have previously reported that mice fed a 54% SFA-rich HFD develop neuropathy by 16 weeks of age, while control mice fed a SD 10% fat chow diet do not develop neuropathy (Hinder et al., 2017). Similarly, in this study we found that mice fed a 60% SFA-rich HFD have impaired sural and sciatic NCV by 16 weeks of age (Fig. 1-2, available at https://doi.org/10.1523/JNEUROSCI.3173-18.2019.f1-2). To evaluate the effect of MUFAs on nerve function, mice fed a HFD from 6 to 24 weeks of age were compared with mice fed a HFD from 6 to 16 weeks of age and then changed to a MUFA-rich diet (HFD-MUFA) until 24 weeks of age (Fig. 1*A*). Metabolic phenotyping at the termination of the study revealed that the HFD and HFD-MUFA groups developed glucose intolerance (Fig. 1*B*; $n = 5–8$ mice per condition: mean ± SEM). Both the HFD and HFD-MUFA animals also had increased body weights (Fig. 1*C*; $n = 5–8$ mice per condition: one-way ANOVA, $F_{(2,16)} = 29.21$, $*p < 0.0001$; Tukey's multiple-comparisons test, $*p < 0.0001$ between SD vs HFD and SD vs HFD-MUFA; no statistically significant difference between HFD vs HFD-MUFA) as well as increased body fat mass and decreased lean mass relative to SD mice (Fig. 1*D*). Despite the same degrees of glucose intolerance and body mass composition, however, neuropathy phenotyping at the termination of the study revealed that consumption of a MUFA-rich HFD for 8 weeks restored normal sural (Fig. 1*E*; $n = 5–8$ mice per condition: one-way ANOVA, $F_{(2,16)} = 37.61$, $p < 0.0001$; Tukey's multiple-comparisons test, $*p = 0.0001$ between SD vs HFD, and HFD vs HFD-MUFA; no statistically significant difference between SD vs HFD-MUFA) and sciatic NCVs (Fig. 1*F*; $n = 5–8$ mice per condition: one-way ANOVA, $F_{(2,16)} = 41.18$, $p < 0.0001$; Tukey's multiple-comparisons test, $*p = 0.0001$ between SD vs HFD, and HFD vs HFD-MUFA; no statistically significant difference between SD vs HFD-MUFA) relative to the HFD mice. In terms of nerve structure, HFD-MUFA mice also had higher levels of IENFD compared with the HFD mice at 24 weeks (Fig. 1*G*; $n = 5–8$ mice per condition: one-way ANOVA, $F_{(2,16)} = 7.243$, $p = 0.0058$; Tukey's multiple-comparisons test, $\#p = 0.0071$ between

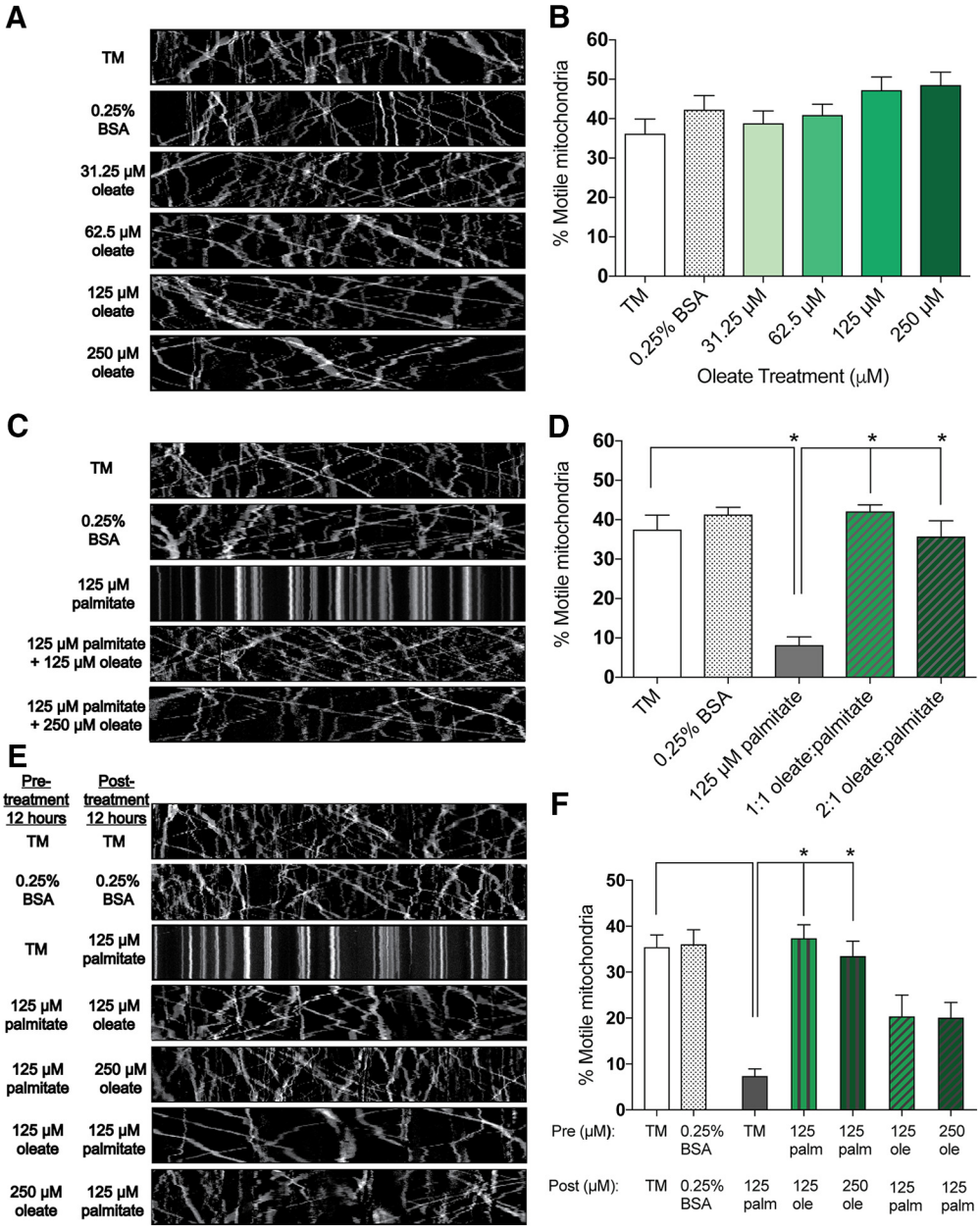

Figure 2. MUFA treatment preserves axonal mitochondrial motility in cultured DRG neurons. ***A***, Kymograph analysis of DRG axons treated for 24 h with TM, vehicle only (0.25% BSA), and varying concentrations (31.25–250 μM) of oleate. ***B***, Percentage of motile mitochondria as observed in ***A***. ***C***, Kymograph analysis of DRG axons treated for 24 h with TM, vehicle only (0.25% BSA), 125 μM palmitate alone, and 125 μM palmitate with 125 or 250 μM oleate. ***D***, Percentage of motile mitochondria as observed in ***C***. ***E***, Kymograph analysis of DRG neurons treated for 24 h with TM, vehicle alone (0.25% BSA), pre-treatment (12 h) with 125 μM palmitate followed by post-treatment (12 h) with 125 or 250 μM oleate, or pre-treatment (12 h) with 125 or 250 μM oleate followed by post-treatment (12 h) with 125 μM palmitate. ***F***, Percentage of motile mitochondria as observed in ***E***. All data represent $n = 16–23$ neurons per condition (***A, B***), $n = 18–23$ neurons per condition (***C, D***), and 12–16 neurons per condition (***E, F***): one-way ANOVA with Tukey's multiple-comparisons test. *$p < 0.0001$.

SD vs HFD, &$p = 0.0297$ between HFD vs HFD-MUFA; no statistically significant difference between SD vs HFD-MUFA). These data demonstrate that altering the degree of fatty acid saturation in the HFD murine chow from SFAs to MUFAs reverses peripheral neuropathy without altering glucose tolerance, body weight, or body composition.

MUFA treatment rescues mitochondrial trafficking in SFA-treated DRG neurons

Because neuropathy was reversed in animals fed a MUFA-based HFD diet, we sought to explore the molecular mechanisms underlying the beneficial effect of MUFAs using primary sensory DRG neurons. We previously reported that the SFA palmitate impairs axonal mitochondrial transport in DRG neurons (Rumora et al., 2018), so we first evaluated mitochondrial transport in cultured DRG neurons in the presence of the MUFA oleate. DRG neurons treated with a physiological concentration range (31.25 μM–250 μM) of exogenous oleate showed no change in the percentage of motile mitochondria relative to the vehicle control (0.25% BSA) or TM alone after 24 h (Fig. 2*A*,*B*; $n = 16–23$ neurons per condition: one-way ANOVA, $F_{(5,114)} = 2.035$, $p = 0.0789$; Tukey's multiple-comparisons test, no statistically significant difference between TM vs 0.25% BSA, and 31.25–250 μM

oleate). Consistent with our previous findings, treatment of DRG neurons with 125 μM palmitate significantly reduced the percentage of motile mitochondria (evidenced by straight lines in the kymograph; Fig. 2*C*,*D*), suggesting differential regulation of mitochondrial trafficking by palmitate and oleate. Because coincubation of oleate and palmitate can prevent cell stress induced by palmitate alone (Listenberger et al., 2003; Coll et al., 2008; Kwon et al., 2014), we next treated DRG neurons with equimolar 1:1 mixtures of oleate and palmitate (at physiologically relevant concentrations of 125 μM each) or with a 2:1 molar ratio of oleate–palmitate (250 μM oleate to 125 μM palmitate). Oleate prevented the reduction in mitochondrial motility conferred by palmitate alone in DRG neurons treated with both ratios of oleate to palmitate (Fig. 2*D*; $n = 18$–23 neurons per condition: one-way ANOVA, $F_{(5,116)} = 21.99$, $p < 0.0001$; Tukey's multiple-comparisons test, $^*p < 0.0001$ between TM vs 125 μM palmitate; no statistically significant difference between TM, 0.25% BSA, 125 μM oleate, 125 μM oleate + 125 μM palmitate, and 250 μM oleate + 125 μM palmitate). These results suggest that oleate prevents palmitate-induced impairment of mitochondrial motility in DRG neurons.

To determine whether oleate rescues mitochondrial motility following inhibition of mitochondrial transport by palmitate, DRG neurons were treated with palmitate for 12 h followed by a 12 h oleate treatment. Although the 12 h 125 μM palmitate treatment reduced mitochondrial motility, subsequent treatment with 125 or 250 μM oleate for 12 h completely restored mitochondrial transport in DRG axons [Fig. 2*E*,*F*; $n = 12$–16 neurons per condition: one-way ANOVA, $F_{(6,93)} = 12.07$, $p < 0.0001$; Tukey's multiple-comparisons test, $^*p < 0.0001$ between TM vs 125 μM palmitate (12 h); no statistically significant difference between TM vs 0.25% BSA, 125 μM palmitate (pre-treatment) + 125 μM oleate (post-treatment), and 125 μM palmitate (pre-treatment) + 250 μM oleate (post-treatment)]. We next determined whether oleate could prevent palmitate-induced impairment of mitochondrial trafficking by pre-treating DRG neurons for 12 h with 125 and 250 μM oleate treatments before a 12 h 125 μM palmitate treatment. Although pre-treatment with oleate did not completely protect DRG neurons from a reduction of mitochondrial transport conferred by palmitate, the percentage of motile mitochondria in DRG neurons pre-treated with oleate was considerably higher than in DRG neurons treated with 125 μM palmitate alone. These data suggest that oleate and palmitate differentially regulate molecular mechanisms involved in axonal mitochondrial transport and that oleate can restore mitochondrial transport after palmitate treatment.

MUFA treatment prevents DRG neuronal mitochondrial depolarization

Impaired mitochondrial transport in palmitate-treated DRG neurons is associated with a loss in MMP during mitochondrial depolarization (Miller and Sheetz, 2004; Rumora et al., 2018, 2019), so we next stained mito-GFP-transfected DRG neurons with TMRM, a fluorophore dependent on MMP, to determine whether oleate prevents palmitate-induced mitochondrial depolarization. Whereas DRG neurons treated with 125 μM palmitate exhibited diffuse TMRM staining in axonal mitochondria, indicating a loss in MMP (Fig. 3*B*), DRG neurons treated with TM, 0.25% BSA, and 125–250 μM oleate retained punctate red TMRM staining that colocalized with the green mito-GFP signal in the merged image (Fig. 3*A*,*C*). Interestingly, a 1:1 equimolar mixture of oleate and palmitate retained TMRM staining in axonal mitochondria (Fig. 3*D*), demonstrating a mito-protective effect of oleate in preventing palmitate-induced mitochondrial depolarization. Quantitation of TMRM staining showed a significant threefold increase in percentage of depolarized mitochondria in palmitate-treated neurons that was abolished by the presence of oleate (Fig. 3*E*; $n = 31$–35 neurons per condition: one-way ANOVA, $F_{(5,196)} = 13.35$, $p < 0.0001$; Tukey's multiple-comparisons test, $^*p < 0.0001$ between TM vs 125 μM palmitate; no statistically significant difference between TM vs 0.25% BSA, 125 μM oleate, 250 μM oleate, and 125 μM oleate + 125 μM palmitate). These data indicate that oleate prevents mitochondrial depolarization in the presence of palmitate.

MUFA treatment prevents decreases in ATP production and DRG neuronal apoptosis

Because mitochondrial depolarization causes a loss of mitochondrial function and reduction in ATP synthesis (Bagkos et al., 2014; Zorova et al., 2018), we next evaluated the ATP level in treated 50B11 DRG neurons using a CellTiter-Glo assay. We found that 62.5–250 μM oleate maintained a basal level of ATP comparable to that of the 0.25% BSA control, whereas 187.5–250 μM palmitate induced a significant reduction in ATP level. This loss of ATP triggered by palmitate was prevented in 1:1 and 2:1 oleate–palmitate mixtures (Fig. 4*A*; $n = 6$ wells of 50B11 neurons per condition: one-way ANOVA, $F_{(11,60)} = 22.63$, $^*p < 0.0001$; Tukey's multiple-comparisons test, $^*p < 0.0001$ between 0.25% BSA vs 187.5 μM palmitate and 250 μM palmitate; no statistically significant difference between 0.25% BSA vs 62.5–250 μM oleate, 62.5–125 μM palmitate, 1:1 oleate + palmitate, and 2:1 oleate + palmitate). Because a loss of MMP can initiate apoptosis (Liao et al., 2011), we also measured activation of pro-apoptotic caspases with a Caspase 3/7-Glo assay in cultured 50B11 DRG neurons treated with 62.5–250 μM oleate, 62.5–250 μM palmitate, and mixtures of oleate and palmitate. Oleate alone did not increase apoptotic signaling in 50B11 DRG neurons, similar to the TM and BSA controls (Fig. 4*B*; $n = 3$ wells of 50B11 neurons per condition: one-way ANOVA, $F_{(13,28)} = 74.27$, $p < 0.0001$; Tukey's multiple-comparisons test, $\#p = 0.0056$ between TM vs 125 μM palmitate, $^*p < 0.0001$ between TM vs 187.5 μM palmitate and 250 μM palmitate; no statistically significant difference between TM vs 0.25% BSA, 62.5–250 μM oleate, 62.5 μM palmitate, 1:1 oleate + palmitate, and 2:1 oleate + palmitate), but treatment with palmitate resulted in a dose-dependent increase in caspase 3/7 activity, with physiological diabetic concentrations of palmitate (250 μM) inducing an approximate fourfold increase in apoptotic signaling. Conversely, treating cells with an equimolar or 2:1 oleate–palmitate mixture completely prevented apoptosis in 50B11 DRG neurons (Fig. 4*B*). These results indicate that oleate protects mitochondrial function and prevents apoptosis in palmitate-treated DRG neurons.

MUFA treatment induces axonal lipid droplet formation

Given that oleate is reported to protect mitochondrial function via the synthesis of triglycerides (Kwon et al., 2014) and formation of intracellular lipid droplets (Listenberger et al., 2003), we evaluated whether oleate triggers intracellular lipid droplet formation in DRG axons. Primary DRG neurons transfected with mito-GFP were treated with palmitate, oleate, or a mixture of both fatty acids for 24 h and stained with Nile red dye to visualize intra-axonal lipid droplets. We then quantified the number of lipid droplets per axon (red images) as well as the number of lipid droplets interacting with green mitochondria (Fig. 5*A*–*E*, yellow in merged images). Although palmitate treatment did not stimulate axonal lipid droplet formation or an increase in lipid drop-

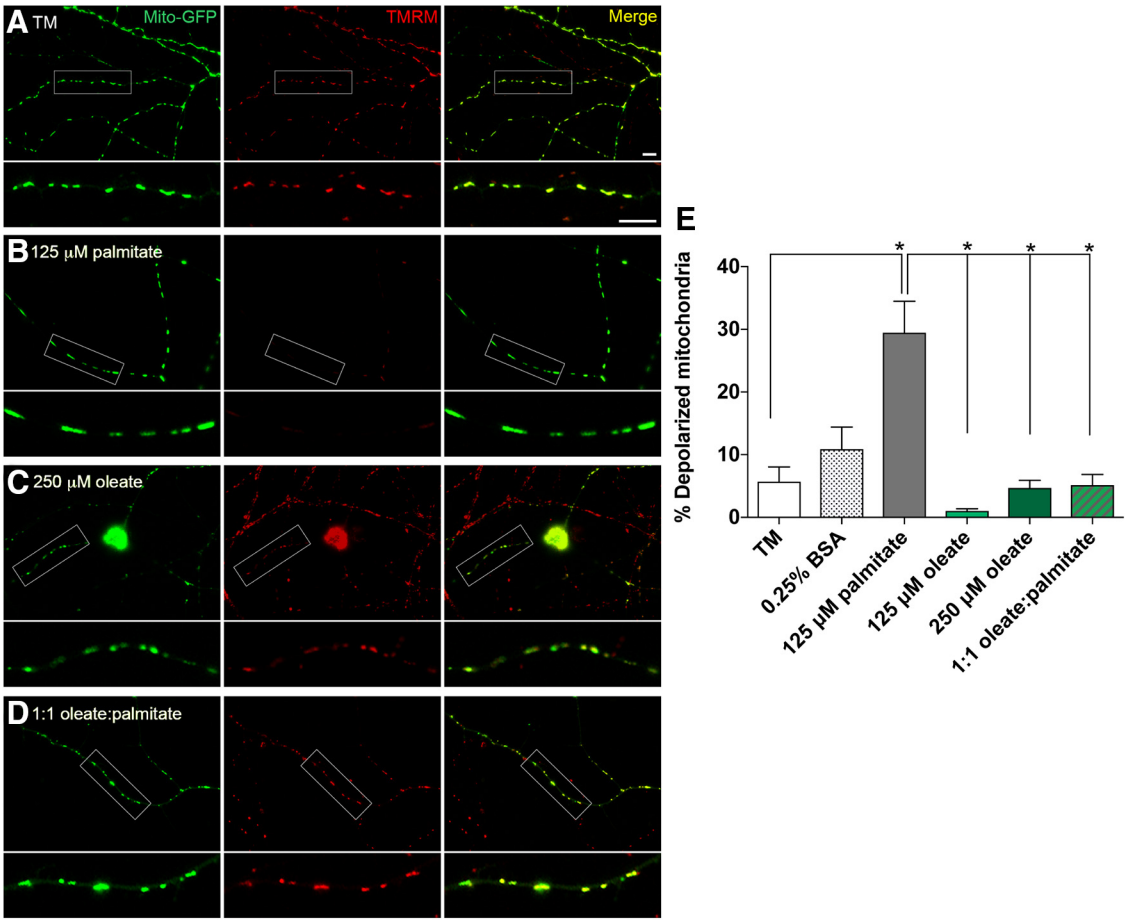

Figure 3. MUFA treatment preserves and protects DRG neuronal MMP. Fluorescence microscopy imaging of DRG neurons expressing mito-GFP that were stained with TMRM dye specific for polarized mitochondrial membranes, following treatment with TM (***A***), 125 μM palmitate (***B***), 250 μM oleate (***C***), or a mix of 125 μM palmitate and oleate (***D***). Green signal (mito-GFP) indicates mitochondria, red signal (TMRM) indicates mitochondria with membrane potential, and yellow signal (Merge) shows overlap of mito-GFP and TMRM signals indicative of polarized mitochondria. Scale bars represent 10 μM. ***E***, Percentage of depolarized mitochondria as shown in ***A***–***D***; i.e., mitochondria fluorescing green (mito-GFP) but lacking red TMRM signal, as a percentage of total mitochondria. All data represent $n = 31$–35 neurons per condition: one-way ANOVA with Tukey's multiple-comparisons test. *$p < 0.0001$.

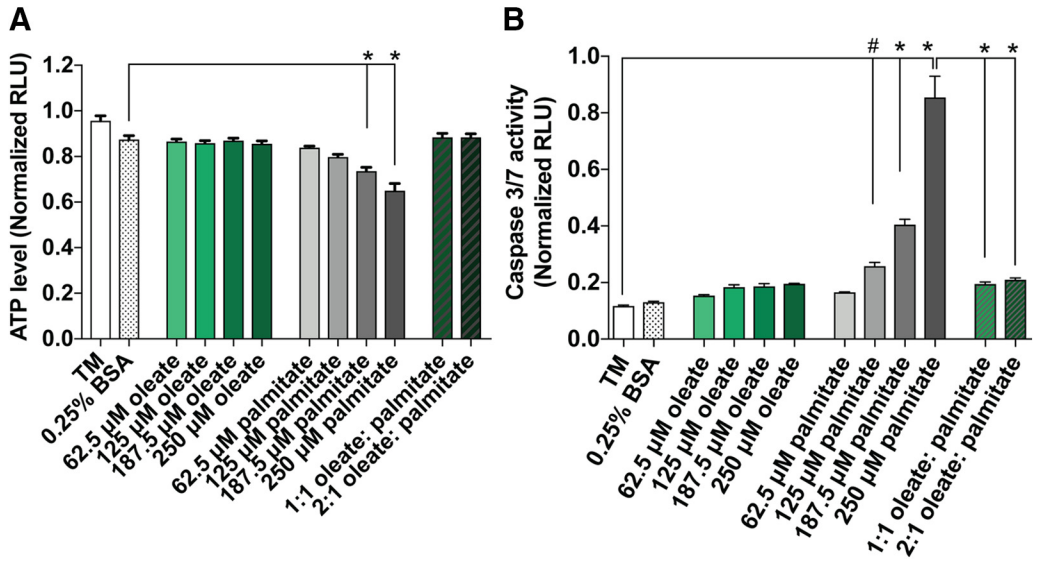

Figure 4. MUFA treatment prevents ATP production decreases and apoptotic signaling induced by palmitate. ***A***, Relative ATP production (RLU) as measured by CellTiter-Glo assay in 50B11 DRG neuronal cells treated for 24 h with TM, vehicle alone (0.25% BSA), varying concentrations (62.5–250 μM) of oleate and palmitate alone, or either 125 or 250 μM oleate mixed with 125 μM palmitate. Data represent mean ± SEM from $n = 6$ wells of 50B11 neurons per condition: one-way ANOVA with Tukey's multiple-comparisons test. $p < 0.0001$ (***B***) Relative caspase 3/7 activity (RLU) as measured by Caspase 3/7-Glo assay in 50B11 DRG neuronal cells treated with conditions identical to those in ***A***. Data represent mean ± SEM from $n = 3$ wells of 50B11 neurons per condition: one-way ANOVA with Tukey's multiple-comparisons test. *$p < 0.0001$ and #$p < 0.0056$.

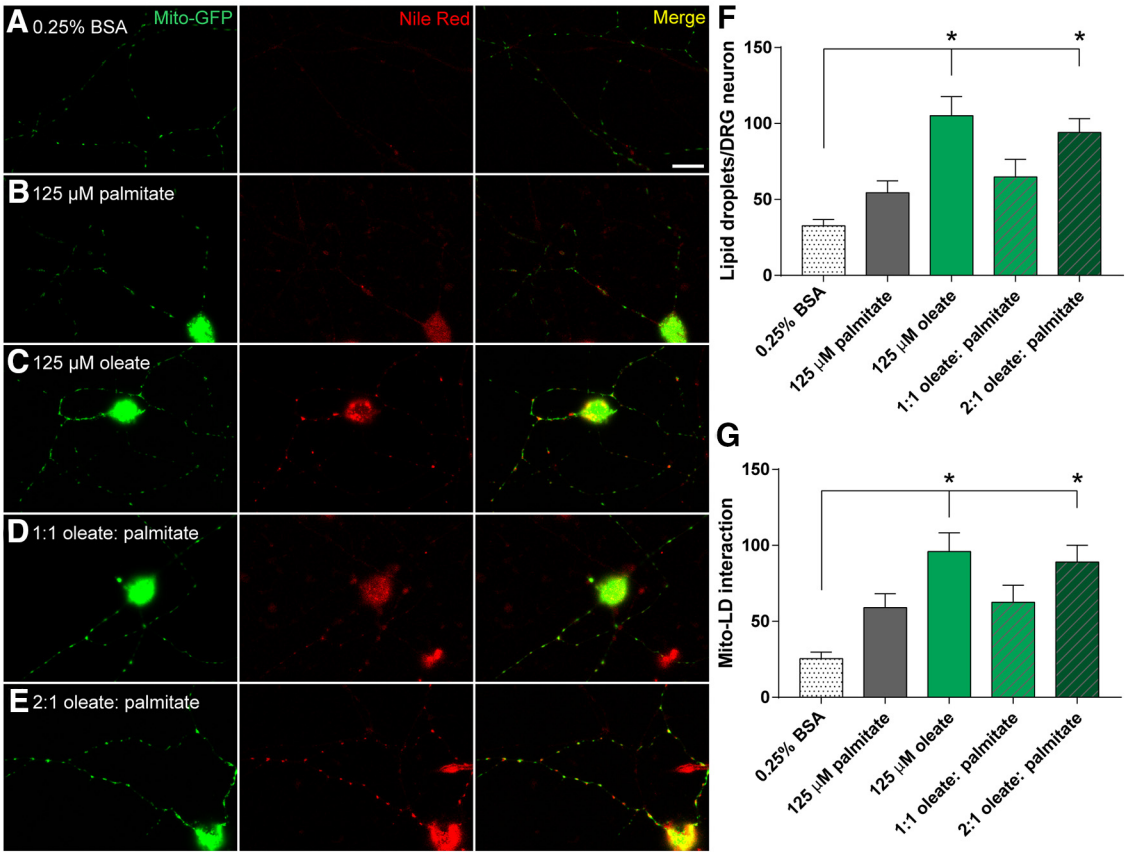

Figure 5. MUFA treatment induces axonal lipid droplet formation in DRG neurons. Fluorescence microscopy of cultured DRG neurons expressing mito-GFP (green puncta) and stained with lipid droplet-specific Nile red (red puncta), following treatment with vehicle alone (0.25% BSA; ***A***), 125 μM palmitate (***B***), or oleate alone (***C***), or 125 μM palmitate mixed with 125 μM (***D***) or 250 μM oleate (***E***). Yellow puncta (Merged signal) indicates colocalization between mitochondria and lipid droplets in DRG axons. Scale bars represent 20 μM. ***F***, Number of lipid droplets (red puncta as stained by Nile red) per DRG neuron as shown in ***A***–***E***. $n = 20-47$ neurons per condition: one-way ANOVA with Tukey's multiple-comparisons test. $^*p < 0.0001$. ***G***, Number of mitochondria colocalizing with lipid droplets (yellow puncta in Mito-GFP/Nile red Merge) per DRG neuron as shown in ***A***–***E***. $n = 20-37$ neurons per condition: one-way ANOVA with Tukey's multiple-comparisons test. $^*p < 0.0001$.

let number in DRG neurons relative to the 0.25% BSA control (Fig. 5*A*,*B*), oleate-treated DRG neurons exhibited increased numbers of punctate red lipid droplets in DRG axons (Fig. 5*C*,*D*). This oleate-induced increase in lipid droplet number was also seen in the presence of palmitate at a 2:1 ratio (Fig. 5*E*); however, a 1:1 ratio of oleate and palmitate did not lead to a significant increase in lipid droplet number (Fig. 5*F*; $n = 20-47$ neurons per condition: one-way ANOVA, $F_{(5,182)} = 10.28$, $p < 0.0001$; Tukey's multiple-comparisons test, $^*p < 0.0001$ between 0.25% BSA vs 125 μM oleate and 2:1 oleate + palmitate; no statistically significant difference between 0.25% BSA vs 125 μM palmitate, and 1:1 oleate + palmitate). Likewise, the number of mitochondria interacting with lipid droplets was significantly higher in cells treated with oleate alone or the 2:1 oleate–palmitate mixture (Fig. 5*G*; $n = 20-37$ neurons per condition: one-way ANOVA, $F_{(5,165)} = 7.528$, $p < 0.0001$; Tukey's multiple-comparisons test, $^*p < 0.0001$ between 0.25% BSA vs 125 μM oleate and 2:1 oleate + palmitate; no statistically significant difference between 0.25% BSA vs 125 μM palmitate, and 1:1 oleate + palmitate). These effects of oleate on lipid droplet formation and number of mitochondria-lipid droplet interactions may represent a mechanism underlying the mito-protective effects of oleate in DRG neurons.

Discussion

The current study demonstrated that a SFA-rich HFD produced neuropathy, whereas dietary intervention with a MUFA-rich HFD restored normal nerve function. Because nerve function depends on axonal mitochondrial ATP production, we further showed that the MUFA oleate prevented impairment of mitochondrial axonal transport by the SFA palmitate in DRG axons, and that oleate maintained axonal MMP and ATP production relative to DRG neurons treated with palmitate alone. Protection of mitochondrial function by oleate was associated with formation of intra-axonal lipid droplets that sequester palmitate, preventing intracellular lipotoxicity. These data suggest that the degree of dietary fatty acid saturation plays a regulatory role in neuropathy.

Mice were fed a lard-based 60% SFA-rich HFD, and by 16 weeks of age were obese with insulin resistance and impaired glucose tolerance relative to mice fed standard chow. This murine model parallels findings in man where prediabetes and T2D are associated with diets rich in SFAs. In a meta-analysis of 19 cross-sectional, 12 prospective, and two nested case-control studies, subjects consuming a Western diet had a 41% increased risk of T2D compared with subjects on a healthy diet (McEvoy et al., 2014). In a study of the interplay between genetic and lifestyle behavioral factors on the risk of T2D in European populations (the EPIC-InterAct study), a case-cohort analysis of 12,403 T2D subjects compared with 16,154 nondiabetic subjects revealed plasma even-chain SFAs strongly correlate with incident T2D. Of these SFAs, palmitic acid, produced by the liver in response to the Western diet, had the highest odds ratio [1.26 (1.15–1.37); Fo-

rouhi et al., 2014]. We previously reported that dietary obesity coupled with impaired glucose tolerance secondary to insulin resistance are the main metabolic drivers of neuropathy in four human clinical studies: a 4000 subject Chinese cohort (Callaghan et al., 2018), a 1445 subject Danish cohort (Andersen et al., 2018), and two separate American cohorts including 102 subjects with a mean age of 52 years (Callaghan et al., 2016b) and 2383 elderly subjects with a mean age of 73 years (Callaghan et al., 2016a). Like their human counterparts, obese and insulin resistant prediabetic mice develop neuropathy, with reduced sural and sciatic NCVs and decreased IENFDs (Hinder et al., 2017; Callaghan et al., 2018), providing an ideal animal model to study the role of dietary fatty acid saturation in neuropathy pathogenesis.

We recently reported normal nerve function in mice switched from a HFD to a standard low fat diet (Hinder et al., 2017). To evaluate whether the beneficial effects of dietary reversal on neuropathy is secondary to the degree of dietary fatty acid saturation, we switched animals from a 60% SFA-rich HFD to a 60% MUFA-rich HFD. We selected this paradigm because MUFAs exhibit a greater rate of oxidation compared with polyunsaturated fatty acids (PUFAs) or SFAs *in vivo* (Jones et al., 1985, 2008; McCloy et al., 2004). The change to a MUFA-rich HFD had no impact on glycemic status, body composition, or body weight, but restored normal sural and sciatic NCVs and IENFDs. This reversal of neuropathy progression suggests that fatty acid saturation, not prediabetes, is the main factor underlying neuropathy progression in HFD-fed obese mice. Partial restoration of nerve function is also seen in diabetic rodent models fed a HFD supplemented with Menhaden oil containing mixtures of PUFAs (Shevalye et al., 2015; Yorek et al., 2017; Coppey et al., 2018; Davidson et al., 2018). However, supplementation with MUFA-rich olive oil did not restore nerve function in obese rats (Coppey et al., 2018). These alternative results may be because of intrinsic differences in lipid metabolism between mice and rats (Menahan and Sobocinski, 1983; Yin et al., 2012) or to fundamental differences in the HFD paradigms. MUFA levels in our chow were 17% higher than in the olive oil supplement, suggesting that a higher MUFA–SFA ratio may restore nerve function (Fig. 1-1, available at https://doi.org/10.1523/JNEUROSCI.3173-18.2019.f1-1). We also focused on neural changes occurring in response to MUFAs earlier in the course of dyslipidemia and neuropathy, between 16 and 24 weeks of age compared with 28–60 weeks of age in the Coppey et al. (2018) study. These data collectively suggest that MUFAs may be an effective early intervention for neuropathy.

Similar findings in prediabetes and T2D rodent models demonstrate that PUFAs improved neuropathy despite persistent hyperglycemia (Yorek et al., 2017). These preclinical data align with National Health and Nutrition Examination Survey reports where the dietary intake of PUFAs associates with lower incident neuropathy (Tao et al., 2008), and EPIC-InterAct study results where dietary PUFAs from plant sources inversely associate with incident T2D (Forouhi et al., 2016). A 12-month study of dietary ω-3 PUFA supplementation in type 1 diabetic subjects showed no change in sensory function or NCVs (Lewis et al., 2017). In contrast, three small studies using different outcome measures and PUFA doses reported improved neuropathy in T2D subjects (Jamal and Carmichael, 1990; Keen et al., 1993; Okuda et al., 1996). These reports, along with the Yorek (2018) laboratory data and our preclinical data, strongly support future contemporary trials evaluating the clinical utility of dietary MUFAs and PUFAs for neuropathy.

To understand the mechanisms underlying fatty acid saturation and nerve function, we evaluated the impact of MUFAs and SFAs on mitochondrial function in DRG sensory neurons. Mitochondria are synthesized in DRG cell bodies (Chang and Reynolds, 2006) and distributed throughout the length of the axon via axonal transport to provide the ATP required for normal nerve function (Kiryu-Seo et al., 2010). We recently showed that physiological concentrations of the SFA palmitate significantly reduced axonal mitochondrial trafficking in DRG neurons (Rumora et al., 2018, 2019); therefore, we assessed how palmitate and the MUFA oleate differentially regulate mitochondrial axonal transport and function in DRG neurons. The human serum metabolome contains 66–122 μM palmitate and 49–122 μM oleate (Psychogios et al., 2011), whereas C57BL/6J mice exhibit up to 250 μM palmitate and 80 μM oleate (Eguchi et al., 2012). Because the concentration of palmitate and oleate in diabetic humans and mice is likely to exceed this concentration range, we used physiological concentrations of palmitate or oleate ranging from 31.25 to 250 μM.

Oleate restored mitochondrial trafficking in palmitate-treated DRG axons. As trafficking is dependent on MMP (Miller and Sheetz, 2004; Koshkin et al., 2008), we showed that palmitate prompted mitochondrial depolarization, whereas oleate restored mitochondrial function. We also observed apoptosis in palmitate-treated DRG neurons, likely secondary to mitochondrial depolarization and decreased intracellular ATP synthesis (Liao et al., 2011; Bagkos et al., 2014; Zorova et al., 2018). Oleate prevented apoptosis by restoring intracellular ATP levels in palmitate-treated DRG neurons. Our findings agree with previous work demonstrating palmitate-induced loss of MMP and subsequent apoptosis in pancreatic cells (Koshkin et al., 2008). In pancreatic cells and podocytes, palmitate mitotoxicity is prevented by exposure to oleate (Maedler et al., 2003; Koshkin et al., 2008; Xu et al., 2015), and MUFAs protect skeletal muscle cells, adipocytes, and hepatocytes from SFA lipotoxicity (Coll et al., 2008; Ricchi et al., 2009; Peng et al., 2011; Finucane et al., 2015). These reports support our data showing that MUFAs restore mitochondrial function in SFA-treated DRG neurons by maintaining normal MMP, ATP levels, and axonal trafficking.

To further understand the beneficial effects of MUFAs, we evaluated whether intra-axonal lipid droplet formation in DRG axons prevents SFA-mediated lipotoxicity. Gene expression profiles of MUFA-treated cells reveal an upregulation of genes related to lipid synthesis pathways (Das et al., 2010; Yuzefovych et al., 2010), and MUFAs upregulate diacylglycerol acyltransferase expression, resulting in accumulation of neutral triglycerides (Das et al., 2010; Kwon et al., 2014), which trigger the formation and expansion of intracellular lipid droplets that store excess SFAs and prevent SFA lipotoxicity (Listenberger et al., 2003; Peng et al., 2011). Lipid droplet formation occurred in cultured DRG axons treated with oleate and oleate/palmitate mixtures, suggesting that MUFAs trigger lipid droplet formation and sequester toxic SFAs into triglycerides to prevent cytoplasmic accumulation of deleterious SFAs and subsequent mitochondrial dysfunction. Sequestration of toxic SFAs into lipid droplets also prevents accumulation of metabolic lipotoxic intermediates, like ceramides, that induce apoptotic signaling (Senkal et al., 2017). Mitochondria associated with lipid droplets also have increased electron transport and ATP synthesis (Benador et al., 2018). Interestingly, lipid droplet formation in the oleate/palmitate mixtures was concentration dependent (Ma et al., 2011; Yenuganti et al., 2016), appearing only at 250 μM oleate, suggesting alternative beneficial effects of low oleate concen-

trations. Oleate increases β-III tubulin expression in neurons (Ghareghani et al., 2017), a protein essential for microtubule formation for organellar trafficking in neurons, and can enhance fatty acid oxidation through a mitochondrial-dependent pathway (Lim et al., 2013).

Overall, we report that mice fed a SFA-rich HFD develop obesity, prediabetes, and neuropathy, reflecting the development of neuropathy in man, while a MUFA-rich HFD reverses neuropathy progression and restores nerve function. The MUFA oleate prevents the impairment of mitochondrial transport and function induced by the SFA palmitate *in vitro*, likely through the formation of intra-axonal lipid droplets. Our work strongly supports dietary intervention for treatment of neuropathy, and provides rationale for a clinical trial of MUFA-rich oils to treat neuropathy in prediabetes and T2D patients.

References

Andersen ST, Witte DR, Dalsgaard EM, Andersen H, Nawroth P, Fleming T, Jensen TM, Finnerup NB, Jensen TS, Lauritzen T, Feldman EL, Callaghan BC, Charles M (2018) Risk factors for incident diabetic polyneuropathy in a cohort with screen-detected type 2 diabetes followed for 13 years: ADDITION-denmark. Diabetes Care 41:1068–1075.

Bagkos G, Koufopoulos K, Piperi C (2014) A new model for mitochondrial membrane potential production and storage. Med Hypotheses 83:175-181.

Benador IY, Veliova M, Mahdaviani K, Petcherski A, Wikstrom JD, Assali EA, Acín-Pérez R, Shum M, Oliveira MF, Cinti S, Sztalryd C, Barshop WD, Wohlschlegel JA, Corkey BE, Liesa M, Shirihai OS (2018) Mitochondria bound to lipid droplets have unique bioenergetics, composition, and dynamics that support lipid droplet expansion. Cell Metab 27:869–885.e6.

Burhans MS, Flowers MT, Harrington KR, Bond LM, Guo CA, Anderson RM, Ntambi JM (2015) Hepatic oleate regulates adipose tissue lipogenesis and fatty acid oxidation. J Lipid Res 56:304–318.

Callaghan BC, Hur J, Feldman EL (2012a) Diabetic neuropathy: one disease or two? Curr Opin Neurol 25:536–541.

Callaghan BC, Little AA, Feldman EL, Hughes RAC (2012b) Enhanced glucose control for preventing and treating diabetic neuropathy. Cochrane Database Syst Rev 6:CD007543.

Callaghan BC, Price RS, Feldman EL (2015) Distal symmetric polyneuropathy: a review. JAMA 314:2172–2181.

Callaghan BC, Xia R, Banerjee M, de Rekeneire N, Harris TB, Newman AB, Satterfield S, Schwartz AV, Vinik AI, Feldman EL, Strotmeyer ES; Health ABC Study (2016a) Metabolic syndrome components are associated with symptomatic polyneuropathy independent of glycemic status. Diabetes Care 39:801–807.

Callaghan BC, Xia R, Reynolds E, Banerjee M, Rothberg AE, Burant CF, Villegas-Umana E, Pop-Busui R, Feldman EL (2016b) Association between metabolic syndrome components and polyneuropathy in an obese population. JAMA Neurol 73:1468–1476.

Callaghan BC, Gao L, Li Y, Zhou X, Reynolds E, Banerjee M, Pop-Busui R, Feldman EL, Ji L (2018) Diabetes and obesity are the main metabolic drivers of peripheral neuropathy. Ann Clin Transl Neurol 5:397–405.

Capel F, Cheraiti N, Acquaviva C, Hénique C, Bertrand-Michel J, Vianey-Saban C, Prip-Buus C, Morio B (2016) Oleate dose-dependently regulates palmitate metabolism and insulin signaling in C2C12 myotubes. Biochim Biophys Acta 1861:2000–2010.

Chang DT, Reynolds IJ (2006) Mitochondrial trafficking and morphology in healthy and injured neurons. Prog Neurobiol 80:241–268.

Chen W, Mi R, Haughey N, Oz M, Höke A (2007) Immortalization and characterization of a nociceptive dorsal root ganglion sensory neuronal line. J Peripher Nerv Syst 12:121–130.

Cheng HT, Dauch JR, Hayes JM, Yanik BM, Feldman EL (2012) Nerve growth factor/p38 signaling increases intraepidermal nerve fiber densities in painful neuropathy of type 2 diabetes. Neurobiol Dis 45:280–287.

Coll T, Eyre E, Rodríguez-Calvo R, Palomer X, Sánchez RM, Merlos M, Laguna JC, Vázquez-Carrera M (2008) Oleate reverses palmitate-induced insulin resistance and inflammation in skeletal muscle cells. J Biol Chem 283:11107–11116.

Coppey L, Davidson E, Shevalye H, Torres ME, Yorek MA (2018) Effect of dietary oils on peripheral neuropathy-related endpoints in dietary obese rats. Diabetes Metab Syndr Obes 11:117–127.

Cortez M, Singleton JR, Smith AG (2014) Glucose intolerance, metabolic syndrome, and neuropathy. Handb Clin Neurol 126:109–122.

Das SK, Mondal AK, Elbein SC (2010) Distinct gene expression profiles characterize cellular responses to palmitate and oleate. J Lipid Res 51: 2121–2131.

Davidson EP, Coppey LJ, Shevalye H, Obrosov A, Yorek MA (2018) Effect of dietary content of menhaden oil with or without salsalate on neuropathic endpoints in high-fat-fed/low-dose streptozotocin-treated Sprague Dawley rats. J Diabetes Res 2018:2967127.

De Vos KJ, Sheetz MP (2007) Visualization and quantification of mitochondrial dynamics in living animal cells. Methods Cell Biol 80:627–682.

De Vos KJ, Sable J, Miller KE, Sheetz MP (2003) Expression of phosphatidylinositol (4,5) bisphosphate-specific pleckstrin homology domains alters direction but not the level of axonal transport of mitochondria. Mol Biol Cell 14:3636–3649.

De Vos KJ, Chapman AL, Tennant ME, Manser C, Tudor EL, Lau KF, Brownlees J, Ackerley S, Shaw PJ, McLoughlin DM, Shaw CE, Leigh PN, Miller CCJ, Grierson AJ (2007) Familial amyotrophic lateral sclerosis-linked SOD1 mutants perturb fast axonal transport to reduce axonal mitochondria content. Hum Mol Genet 16:2720–2728.

Ducheix S, Montagner A, Polizzi A, Lasserre F, Régnier M, Marmugi A, Benhamed F, Bertrand-Michel J, Mselli-Lakhal L, Loiseau N, Martin PG, Lobaccaro JM, Ferrier L, Postic C, Guillou H (2017) Dietary oleic acid regulates hepatic lipogenesis through a liver X receptor-dependent signaling. PLOS ONE 12:e0181393.

Eguchi K, Manabe I, Oishi-Tanaka Y, Ohsugi M, Kono N, Ogata F, Yagi N, Ohto U, Kimoto M, Miyake K, Tobe K, Arai H, Kadowaki T, Nagai R (2012) Saturated fatty acid and TLR signaling link â cell dysfunction and islet inflammation. Cell Metab 15:518–533.

Finucane OM, Lyons CL, Murphy AM, Reynolds CM, Klinger R, Healy NP, Cooke AA, Coll RC, McAllan L, Nilaweera KN, O'Reilly ME, Tierney AC, Morine MJ, Alcala-Diaz JF, Lopez-Miranda J, O'Connor DP, O'Neill LA, McGillicuddy FC, Roche HM (2015) Monounsaturated fatty acid-enriched high-fat diets impede adipose NLRP3 inflammasome-mediated IL-1â secretion and insulin resistance despite obesity. Diabetes 64:2116–2128.

Forouhi NG, Koulman A, Sharp SJ, Imamura F, Kröger J, Schulze MB, Crowe FL, Huerta JM, Guevara M, Beulens JW, van Woudenbergh GJ, Wang L, Summerhill K, Griffin JL, Feskens EJ, Amiano P, Boeing H, Clavel-Chapelon F, Dartois L, Fagherazzi G, et al. (2014) Differences in the prospective association between individual plasma phospholipid saturated fatty acids and incident type 2 diabetes: the EPIC-InterAct case-cohort study. Lancet Diabetes Endocrinol 2:810–818.

Forouhi NG, Imamura F, Sharp SJ, Koulman A, Schulze MB, Zheng J, Ye Z, Sluijs I, Guevara M, Huerta JM, Kröger J, Wang LY, Summerhill K, Griffin JL, Feskens EJ, Affret A, Amiano P, Boeing H, Dow C, Fagherazzi G, et al. (2016) Association of plasma phospholipid n-3 and n-6 polyunsaturated fatty acids with type 2 diabetes: the EPIC-InterAct case-cohort study. PLoS Med 13:e1002094.

Fraze E, Donner CC, Swislocki AL, Chiou YA, Chen YD, Reaven GM (1985) Ambient plasma free fatty acid concentrations in noninsulin-dependent diabetes mellitus: evidence for insulin resistance. J Clin Endocrinol Metab 61:807–811.

German JB, Dillard CJ (2004) Saturated fats: what dietary intake? Am J Clin Nutr 80:550–559.

Ghareghani M, Zibara K, Azari H, Hejr H, Sadri F, Jannesar R, Ghalamfarsa G, Delaviz H, Nouri E, Ghanbari A (2017) Safflower seed oil, containing oleic acid and palmitic acid, enhances the stemness of cultured embryonic neural stem cells through Notch1 and induces neuronal differentiation. Front Neurosci 11:446.

Greenspan P, Mayer EP, Fowler SD (1985) Nile red: a selective fluorescent stain for intracellular lipid droplets. J Cell Biol 100:965–973.

Hagenfeldt L, Wahren J, Pernow B, Räf L (1972) Uptake of individual free fatty acids by skeletal muscle and liver in man. J Clin Invest 51:2324–2330.

Henique C, Mansouri A, Fumey G, Lenoir V, Girard J, Bouillaud F, Prip-Buus C, Cohen I (2010) Increased mitochondrial fatty acid oxidation is sufficient to protect skeletal muscle cells from palmitate-induced apoptosis. J Biol Chem 285:36818–36827.

Hinder LM, O'Brien PD, Hayes JM, Backus C, Solway AP, Sims-Robinson C,

Feldman EL (2017) Dietary reversal of neuropathy in a murine model of prediabetes and metabolic syndrome. Dis Model Mech 10:717–725.
Jamal GA, Carmichael H (1990) The effect of gamma-linolenic acid on human diabetic peripheral neuropathy: a double-blind placebo-controlled trial. Diabet Med 7:319–323.
Jones PJ, Jew S, AbuMweis S (2008) The effect of dietary oleic, linoleic, and linolenic acids on fat oxidation and energy expenditure in healthy men. Metab Clin Exp 57:1198–1203.
Jones PJ, Pencharz PB, Clandinin MT (1985) Whole body oxidation of dietary fatty acids: implications for energy utilization. Am J Clin Nutr 42:769–777.
Keen H, Payan J, Allawi J, Walker J, Jamal GA, Weir AI, Henderson LM, Bissessar EA, Watkins PJ, Sampson M (1993) Treatment of diabetic neuropathy with γ-linolenic acid: the γ-Linolenic Acid Multicenter Trial Group. Diabetes Care 16:8–15.
Kiryu-Seo S, Ohno N, Kidd GJ, Komuro H, Trapp BD (2010) Demyelination increases axonal stationary mitochondrial size and the speed of axonal mitochondrial transport. J Neurosci 30:6658–6666.
Koshkin V, Dai FF, Robson-Doucette CA, Chan CB, Wheeler MB (2008) Limited mitochondrial permeabilization is an early manifestation of palmitate-induced lipotoxicity in pancreatic beta-cells. J Biol Chem 283:7936–7948.
Kwon B, Lee HK, Querfurth HW (2014) Oleate prevents palmitate-induced mitochondrial dysfunction, insulin resistance and inflammatory signaling in neuronal cells. Biochim Biophys Acta 1843:1402–1413.
Lewis EJH, Perkins BA, Lovblom LE, Bazinet RP, Wolever TMS, Bril V (2017) Effect of omega-3 supplementation on neuropathy in type 1 diabetes: a 12-month pilot trial. Neurology 88:2294–2301.
Liao J, Zhao Q, Han X, Diwu Z (2011) Analyzing cellular apoptosis through monitoring mitochondrial membrane potential changes with JC-10. Biophys J 100:39a.
Lim JH, Gerhart-Hines Z, Dominy JE, Lee Y, Kim S, Tabata M, Xiang YK, Puigserver P (2013) Oleic acid stimulates complete oxidation of fatty acids through protein kinase A-dependent activation of SIRT1-PGC1á complex. J Biol Chem 288:7117–7126.
Listenberger LL, Han X, Lewis SE, Cases S, Farese RV Jr, Ory DS, Schaffer JE (2003) Triglyceride accumulation protects against fatty acid-induced lipotoxicity. Proc Natl Acad Sci U S A 100:3077–3082.
Ma S, Yang D, Li D, Tang B, Yang Y (2011) Oleic acid induces smooth muscle foam cell formation and enhances atherosclerotic lesion development via CD36. Lipids Health Dis 10:53.
Maedler K, Oberholzer J, Bucher P, Spinas GA, Donath MY (2003) Monounsaturated fatty acids prevent the deleterious effects of palmitate and high glucose on human pancreatic-cell turnover and function. Diabetes 52:726–733.
McCloy U, Ryan MA, Pencharz PB, Ross RJ, Cunnane SC (2004) A comparison of the metabolism of eighteen-carbon 13C-unsaturated fatty acids in healthy women. J Lipid Res 45:474–485.
McEvoy CT, Cardwell CR, Woodside JV, Young IS, Hunter SJ, McKinley MC (2014) A posteriori dietary patterns are related to risk of type 2 diabetes: findings from a systematic review and meta-analysis. J Acad Nutr Diet 114:1759–1775.e4.
Menahan LA, Sobocinski KA (1983) Comparison of carbohydrate and lipid metabolism in mice and rats during fasting. Comp Biochem Physiol, B 74:859–864.
Miles JM, Wooldridge D, Grellner WJ, Windsor S, Isley WL, Klein S, Harris WS (2003) Nocturnal and postprandial free fatty acid kinetics in normal and type 2 diabetic subjects: effects of insulin sensitization therapy. Diabetes 52:675–681.
Miller KE, Sheetz MP (2004) Axonal mitochondrial transport and potential are correlated. J Cell Sci 117:2791–2804.
O'Brien PD, Sakowski SA, Feldman EL (2014) Mouse models of diabetic neuropathy. ILAR J 54:259–272.
O'Brien PD, Hinder LM, Rumora AE, Hayes JM, Dauch JR, Backus C, Mendelson FE, Feldman EL (2018) Juvenile murine models of prediabetes and type 2 diabetes develop neuropathy. Dis Model Mech 11: dmm037374.
Oh SS, Hayes JM, Sims-Robinson C, Sullivan KA, Feldman EL (2010) The effects of anesthesia on measures of nerve conduction velocity in male C57Bl6/J mice. Neurosci Lett 483:127–131.
Okuda Y, Mizutani M, Ogawa M, Sone H, Asano M, Asakura Y, Isaka M, Suzuki S, Kawakami Y, Field JB, Yamashita K (1996) Long-term effects of eicosapentaenoic acid on diabetic peripheral neuropathy and serum lipids in patients with type II diabetes mellitus. J Diabetes Complicat 10:280–287.
Peng G, Li L, Liu Y, Pu J, Zhang S, Yu J, Zhao J, Liu P (2011) Oleate blocks palmitate-induced abnormal lipid distribution, endoplasmic reticulum expansion and stress, and insulin resistance in skeletal muscle. Endocrinology 152:2206–2218.
Psychogios N, Hau DD, Peng J, Guo AC, Mandal R, Bouatra S, Sinelnikov I, Krishnamurthy R, Eisner R, Gautam B, Young N, Xia J, Knox C, Dong E, Huang P, Hollander Z, Pedersen TL, Smith SR, Bamforth F, Greiner R, et al. (2011) The human serum metabolome. PLoS One 6:e16957.
Qian F, Korat AA, Malik V, Hu FB (2016) Metabolic effects of monounsaturated fatty acid-enriched diets compared with carbohydrate or polyunsaturated fatty acid-enriched diets in patients with type 2 diabetes: a systematic review and meta-analysis of randomized controlled trials. Diabetes Care 39:1448–1457.
Ricchi M, Odoardi MR, Carulli L, Anzivino C, Ballestri S, Pinetti A, Fantoni LI, Marra F, Bertolotti M, Banni S, Lonardo A, Carulli N, Loria P (2009) Differential effect of oleic and palmitic acid on lipid accumulation and apoptosis in cultured hepatocytes. J Gastroenterol Hepatol 24:830–840.
Rumin J, Bonnefond H, Saint-Jean B, Rouxel C, Sciandra A, Bernard O, Cadoret JP, Bougaran G (2015) The use of fluorescent nile red and BODIPY for lipid measurement in microalgae. Biotechnol Biofuels 8:42.
Rumora AE, Lentz SI, Hinder LM, Jackson SW, Valesano A, Levinson GE, Feldman EL (2018) Dyslipidemia impairs mitochondrial trafficking and function in sensory neurons. FASEB J 32:195–207.
Rumora AE, LoGrasso G, Haidar JA, Dolkowski JJ, Lentz SI, Feldman EL (2019) Chain length of saturated fatty acids regulates mitochondrial trafficking and function in sensory neurons. J Lipid Res 60:58–70.
Russell JW, Golovoy D, Vincent AM, Mahendru P, Olzmann JA, Mentzer A, Feldman EL (2002) High glucose-induced oxidative stress and mitochondrial dysfunction in neurons. FASEB J 16:1738–1748.
Schwarz TL (2013) Mitochondrial trafficking in neurons. Cold Spring Harb Perspect Biol 5:a011304.
Senkal CE, Salama MF, Snider AJ, Allopenna JJ, Rana NA, Koller A, Hannun YA, Obeid LM (2017) Ceramide is metabolized to acylceramide and stored in lipid droplets. Cell Metab 25:686–697.
Sheng ZH (2014) Mitochondrial trafficking and anchoring in neurons: new insight and implications. J Cell Biol 204:1087–1098.
Shevalye H, Yorek MS, Coppey LJ, Holmes A, Harper MM, Kardon RH, Yorek MA (2015) Effect of enriching the diet with menhaden oil or daily treatment with resolvin D1 on neuropathy in a mouse model of type 2 diabetes. Journal of Neurophysiology 114:199–208.
Smith AG, Russell J, Feldman EL, Goldstein J, Peltier A, Smith S, Hamwi J, Pollari D, Bixby B, Howard J, Singleton JR (2006) Lifestyle intervention for pre-diabetic neuropathy. Diabetes Care 29:1294–1299.
Tabák AG, Herder C, Rathmann W, Brunner EJ, Kivimäki M (2012) Prediabetes: a high-risk state for diabetes development. Lancet 379:2279–2290.
Tao M, McDowell MA, Saydah SH, Eberhardt MS (2008) Relationship of polyunsaturated fatty acid intake to peripheral neuropathy among adults with diabetes in the national health and nutrition examination survey (NHANES) 1999 2004. Diabetes Care 31:93–95.
Thörn K, Bergsten P (2010) Fatty acid-induced oxidation and triglyceride formation is higher in insulin-producing MIN6 cells exposed to oleate compared to palmitate. J Cell Biochem 111:497–507.
Vincent AM, Russell JW, Sullivan KA, Backus C, Hayes JM, McLean LL, Feldman EL (2007) SOD2 protects neurons from injury in cell culture and animal models of diabetic neuropathy. Exp Neurol 208:216–227.
Vincent AM, Hayes JM, McLean LL, Vivekanandan-Giri A, Pennathur S, Feldman EL (2009a) Dyslipidemia-induced neuropathy in mice: the role of oxLDL/LOX-1. Diabetes 58:2376–2385.
Vincent AM, Kato K, McLean LL, Soules ME, Feldman EL (2009b) Sensory neurons and schwann cells respond to oxidative stress by increasing antioxidant defense mechanisms. Antioxid Redox Signal 11:425–438.
Wanders AJ, Alssema M, de Koning EJ, le Cessie S, de Vries JH, Zock PL, Rosendaal FR, Heijer MD, de Mutsert R (2017) Fatty acid intake and its dietary sources in relation with markers of type 2 diabetes risk: the NEO study. Eur J Clin Nutr 71:245–251.
Xu S, Nam SM, Kim JH, Das R, Choi SK, Nguyen TT, Quan X, Choi SJ, Chung CH, Lee EY, Lee IK, Wiederkehr A, Wollheim CB, Cha SK, Park KS (2015) Palmitate induces ER calcium depletion and apoptosis in mouse

podocytes subsequent to mitochondrial oxidative stress. Cell Death and Disease 6:e1976.

Yenuganti VR, Viergutz T, Vanselow J (2016) Oleic acid induces specific alterations in the morphology, gene expression and steroid hormone production of cultured bovine granulosa cells. Gen Comp Endocrinol 232: 134–144.

Yin W, Carballo-Jane E, McLaren DG, Mendoza VH, Gagen K, Geoghagen NS, McNamara LA, Gorski JN, Eiermann GJ, Petrov A, Wolff M, Tong X, Wilsie LC, Akiyama TE, Chen J, Thankappan A, Xue J, Ping X, Andrews G, Wickham LA, et al. (2012) Plasma lipid profiling across species for the identification of optimal animal models of human dyslipidemia. J Lipid Res 53:51–65.

Yorek MA (2018) The potential role of fatty acids in treating diabetic neuropathy. Curr Diab Rep 18:86.

Yorek MS, Obrosov A, Shevalye H, Coppey LJ, Kardon RH, Yorek MA (2017) Early vs. late intervention of high fat/low dose streptozotocin treated C57Bl/6J mice with enalapril, á-lipoic acid, menhaden oil or their combination: effect on diabetic neuropathy related endpoints. Neuropharmacology 116:122–131.

Yuzefovych L, Wilson G, Rachek L (2010) Different effects of oleate vs. palmitate on mitochondrial function, apoptosis, and insulin signaling in L6 skeletal muscle cells: role of oxidative stress. Am J Physiol Endocrinol Metab 299:E1096–E1105.

Zorova LD, Popkov VA, Plotnikov EJ, Silachev DN, Pevzner IB, Jankauskas SS, Zorov SD, Babenko VA, Zorov DB (2018) Functional significance of the mitochondrial membrane potential. Biochem (Mosc) Suppl Ser A Membr Cell Biol 12:20–26.